Title

Impact of Tissue Handling and Size Modification on Septal Chondrocyte Viability

Journal

The Laryngoscope, 134(10)

ISSN

0023-852X

Authors

Goshtasbi, Khodayar

Nguyen, Theodore V

Prasad, Karthik R

et al.

Publication Date

2024-10-01

DOI

10.1002/lary.31546

The Laryngoscope

Impact of Tissue Handling and Size Modification on Septal Chondrocyte Viability

Khodayar Goshtasbi, MD; Theodore V. Nguyen, BS; Karthik R. Prasad, MD; Ellen M. Hong, BS; Naya Sterritt; Katelyn K. Dilley, BS; Konrad Kozlowski, BS; Alexis Ha; Brian J.F. Wong, MD, PhD

Introduction: The physical modification of cartilage grafts during rhinoplasty risks chondrocyte death at the margins where the tissue is cut. This study compares chondrocyte viability between diced, scaled, and pate samples in human models, and further computes percent chondrocyte viability as a function of sequential dicing size in a computational model.

Methods: Septal cartilage from 11 individuals was prepared as follows: diced (1 mm cubic), scaled (shaved to <1 mm thickness ~ translucent), pate (0.02 g of scraped cartilage surface), positive control (2 × 2 mm diced), and negative control (2 × 2 mm diced soaked in 70% EtOH). Viability analysis was performed using Live/Dead assay™ and confocal microscopy. Numerical simulation of cartilage dicing in 0.05 mm increments was performed using MATLAB assuming 250 chondrocytes/mm^3 with each average chondrocyte size of 65 μm^2.

Results: Chondrocyte viability was similar between 1 mm diced cartilage, scaled cartilage, and positive control samples ($p > 0.05$). Conversely, pate samples had significantly less viability compared to positive controls, diced samples, and scaled samples (all $p < 0.01$ after Bonferroni correction). Pate samples had similar chondrocyte viability compared to negative controls ($p = 0.36$). On computational modeling, cartilage viability decreased to 50% as the diced sample was cut from 1 mm edge length to 0.7–0.8 mm. Similarly, cartilage viability decreased to 26% at 0.55–0.65 mm, 11% at 0.4–0.5 mm, and <5% at <0.4 mm edge length.

Conclusion: Modifying septal cartilage grafts into 1 mm diced or scaled samples maintains ideal chondrocyte viability whereas pate preparations result in significant chondrocyte death. According to computational analysis, chondrocyte viability sharply decreases as the cartilage is diced below 0.7–0.8 mm.

Key Words: cartilage viability, chondrocyte viability, diced cartilage, rhinoplasty, tissue viability.

Level of Evidence: N/A

***Laryngoscope*, 134:4259–4265, 2024**

INTRODUCTION

Contemporary rhinoplasty techniques rely on septal, auricular, and costal cartilage grafts. Autologous solid cartilage grafts offer the ideal graft material with lower infection and extrusion rates as well as increased longevity.[1] Clinically insignificant volume resorption often in tandem with fibrous tissue replacement has also been noted.[2] Crushing cartilage or placement in regions under high tensile or compressive forces may lead to cartilage volume loss.[2,3] Cartilage crushing is widely used as rigidity/warping is reduced and formation of facets from contracture is minimized.[4,5] Finely diced cartilage for dorsal augmentation has risen in popularity as well, and used primarily for dorsal augmentation, but also as injected micrografts to smooth contours.[6–8]

The viability of chondrocytes in crushed cartilage grafts depends on the severity of cartilage manipulation.[9–11] Kayabasoglu et al. demonstrate superior cell viability in diced auricular cartilage compared to crushed or morselized auricular cartilage grafts in rabbits.[12] Furthermore, Garg et al. demonstrated a continuous decrease in immediate cell viability counts for intact, slightly crushed, moderately, crushed, significantly crushed, and severely crushed septum cartilage.[10] Here, we determine chondrocyte viability in human septum after crushing, dicing, and pate formation using laser scanning confocal microscopy and Live/Dead assay™. In addition, we present a simple numerical model that estimates chondrocyte viability as a function of decreasing cube size via dicing. Chondrocyte injury due to progressively smaller sectioning has not been examined using numerical analysis, and this relationship merits exploration.

METHODS

The study was performed in accordance with the University of California, Irvine Institutional Review Board exemption criteria. Fresh remnant nasal septal cartilage from 11 healthy individuals undergoing rhinoplasty were obtained. The cartilage

From the Department of Otolaryngology-Head and Neck Surgery (K.G., B.J.F.W.), University of California Irvine, Irvine, California, U.S.A.; Beckman Laser Institute (T.V.N., K.R.P., E.M.H., K.K.D., K.K., A.H., B.J.F.W.), University of California Irvine, Irvine, California, U.S.A.; and the School of Biomedical Engineering (N.S., B.J.F.W.), University of California Irvine, Irvine, California, U.S.A.

Editor's Note: This Manuscript was accepted for publication on May 13, 2024.

The authors have no financial relationships or conflicts of interest to disclose.

Portions of this work were presented at the Triological Society Combined Sections Meeting, January 25–27, 2024, West Palm Beach, FL.

Send correspondence to Brian J. F. Wong, Department of Otolaryngology-Head and Neck Surgery, University of California, Irvine, 1002 Health Sciences Road, Irvine, CA 9261. Email: bjwong@uci.edu

DOI: 10.1002/lary.31546

pieces were stripped of perichondrium and placed in normal saline solution. Specimens were kept at ambient temperature and tissue processing was performed on the same day as surgery. The samples were divided into five groups: diced, sliced (i.e., "scales"), pate, positive control, and negative control. Diced cartilage samples were cut to cubes with edge length of 1 mm. Scales were generated by shaving samples into translucent sheets less than 1 mm thick. A 10-blade scalpel scraped the cartilage surface at a 75- to 80-degree angle to collect 0.02 g of "pâté." Positive control was a large 2 × 2 × 2 mm diced sample without any treatment. Negative control was a 2 × 2 × 2 mm diced sample soaked in 70% EtOH for 2 h and expected to have maximum chondrocyte death. All measurements were performed using a Vernier caliper to confirm uniformity.

Viability analysis was performed within a day of surgery using a Live/Dead assay (Molecular Probes Inc, Eugene, Oregon) in conjunction with laser scanning confocal microscopy (Meta 510; Carl Zeiss LSM, Peabody, Massachuesetts), similar to previously published methods.[13–16] After the initial sectioning, all samples were washed three times with Hank's Balanced Salt Solution (HBSS). The viability assay was performed using green-fluorescent calcein-AM and red-fluorescent ethidium homodimer-1 stains. Stock solution was created by mixing 50 μL calcein (1 μg/μL) with 50 μL of dimethylsulfoxide (DMSO). Prior to staining, 1 mL of calcein stock solution was mixed with 99 μL of HBSS. A 1 μg/μL ethidum homodimer working solution was created by mixing 1 mg of ethidium homodimer with 1 mL of DMSO. Each sample group was mixed with 2 μL of 0.1 μg/μL Calcein, 10 μL of 1 μg/μL Ethidium Homodimer, and 988 μL of HBSS. Samples were vortexed for 30 s, and then incubated at 37°C for 4 min. After the incubation, samples were washed with 1 mL of HBSS and allowed to incubate for an additional 5–10 min. Samples were washed once more with 1 mL of HBSS before imaging.

Specimens were then examined with a laser-scanning confocal microscope employing a 488 nm argon laser excitation source at 10× magnification. When used as a "live" stain, calcein AM serves as an indicator of cells which have intact cell membranes and esterase activity.[17] It is a fluorogenic esterase substrate hydrolyzed by living cells to yield a green fluorescent product.[18] Ethidium homodimer permeates cells with compromised membranes, where it binds to RNA with high affinity and weakly binds to DNA, therefore it serves as a proxy for cell death. The green and red fluorescent signals produced by these two dyes were collected independently using two separate color channels. All images were transferred via portable media to another computer for analysis.

Digital images were evaluated via ImageJ. Post-imaging live/dead counts were manually determined by two trained researchers who were blinded to specimen preparation. Cell viability was determined by dividing the number of live cells by the number of total cells for each image. The scores of the two counters were then averaged within each preparation group to determine chondrocyte viability. Interclass correlation coefficient (ICC) was calculated between the two counters to determine inter-rater reliability. The statistical tests were performed using IBM SPSS (v29, Armonk, MN). Statistical significance for the Live/Dead assay was performed using one-way ANOVA to compare each manipulation group against control groups. The P values were reported for each comparison and significance was determined using Bonferroni's correction ($p < .01$).

Simulation of the dicing was performed using code written in MATLAB (MathWorks Inc, Natick, MA). A cube with a length of 1 mm was created with 250 equal sub-cubes. Previous literature has shown that the density of chondrocytes in septal cartilage is 250 chondrocytes/mm^3 with each chondrocyte having an average radius of 30 μm.[19–21] The center of each sub-cube was populated with spheres with a radius of 30 μm to represent individual chondrocytes equidistant from one another. To simulate dicing of cartilage in smaller sizes, the cube was serially downsized by 0.05 mm increments. Spheres outside the downsized cube or transecting any of the six planes of the cube were manually colored to red to represent dead chondrocytes. Those remaining within the cube were thus "alive" and colored green. In other words, each serial downsizing highlighted structural differences with red spheres outside the downsized cube or transecting any of the six planes of the cube as dead chondrocytes, and green spheres inside the cube as alive chondrocytes. The percentage of "alive" (e.g., non-transected) chondrocytes at each size increment were calculated as the number of alive chondrocytes within the cube, represented by green spheres, divided by the total sum of 250 chondrocytes within the initial 1 mm^3 cube. Graphs were created in Microsoft Excel.

RESULTS

Nasal septal cartilage from 11 individuals with a mean age of 29.4 ± 10.8 years (range 19–51 years) undergoing primary rhinoplasty were collected. There was no association between age and percent viable cells among positive controls ($p = 0.75$). Figure 1 shows examples of live dead analysis (and green vs. red color differentiation) of each type of sample under electron microscopy. The ICC between the independently counted number of viable chondrocytes had an interclass correlation ICC of 0.949, suggesting close agreements. Figure 2 demonstrates the averaged percent chondrocyte viability counts among the five groups (diced, scaled, pate, positive control, and negative control), which are 60.6 ± 18.1 for alive controls, 1.4 ± 1.5 for dead controls, 67.9 ± 1.5 for diced samples, 46.3 ± 20.0 for scale samples, and 18.2 ± 17.2 for pate samples. In comparing the chondrocyte viability between the five groups, one-way ANOVA showed significant differences in chondrocyte viability in at least two groups [$F(4, 23) = 18.275$, $p < 0.001$]. Post hoc comparison using Bonferroni correction showed that, as expected, alive control had significantly more viable chondrocytes than dead (formalin) controls ($p < 0.001$). Scale and diced samples both had similar viability to alive samples ($p > 0.05$). However, pate samples had significantly lower viability compared to alive samples ($p < 0.001$) and similar viability to negative controls ($p = 0.440$). The post hoc analyses are summarized in Table I.

Computational modeling of diced cartilage preparations was performed with sequential analysis of chondrocyte viability with incremental size decreases (Figs. 3 and 4). The figures demonstrate a dramatic decrease in percent viable cells as the diced cubes' edges are continuously cut in 0.05 mm increments. As demonstrated in figures 3 and 4, a cube edge length of 1 mm corresponded to 100% chondrocyte viability, whereas 0.7–0.8 mm corresponded to 50% chondrocyte viability; at cube edge lengths of 0.55–0.65 mm, 25.6% of chondrocytes were viable; at lengths of 0.4–0.5 mm, 10.8% of chondrocytes were viable; and at cube edge lengths of <0.4 mm, less than 5% of chondrocytes were deemed viable. These results are also demonstrated in Figure 5 in a graphic manner,

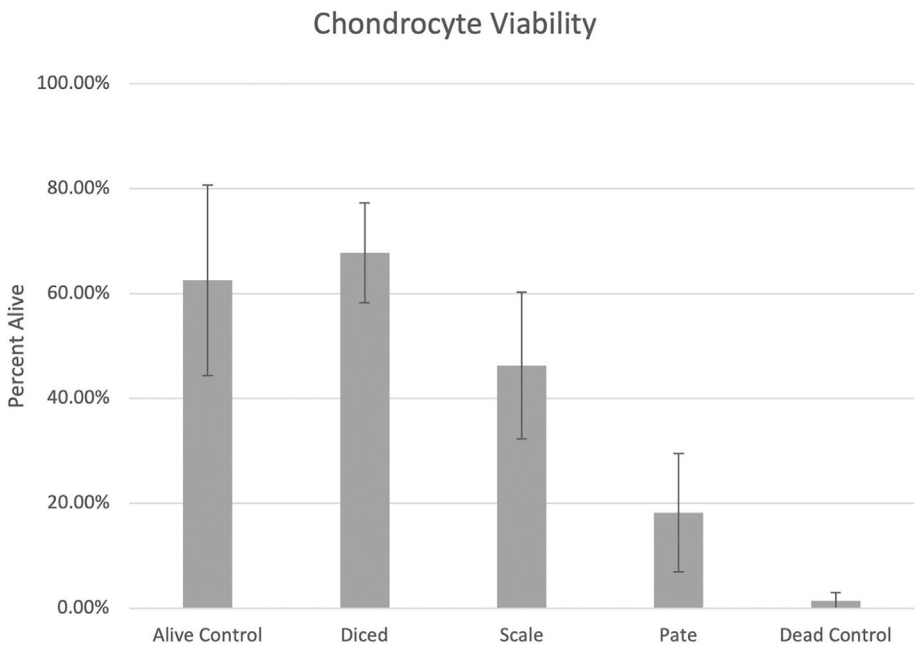

Fig. 1. Chondrocyte viability of different surgical preparations of cartilage versus control including standard deviation bars.

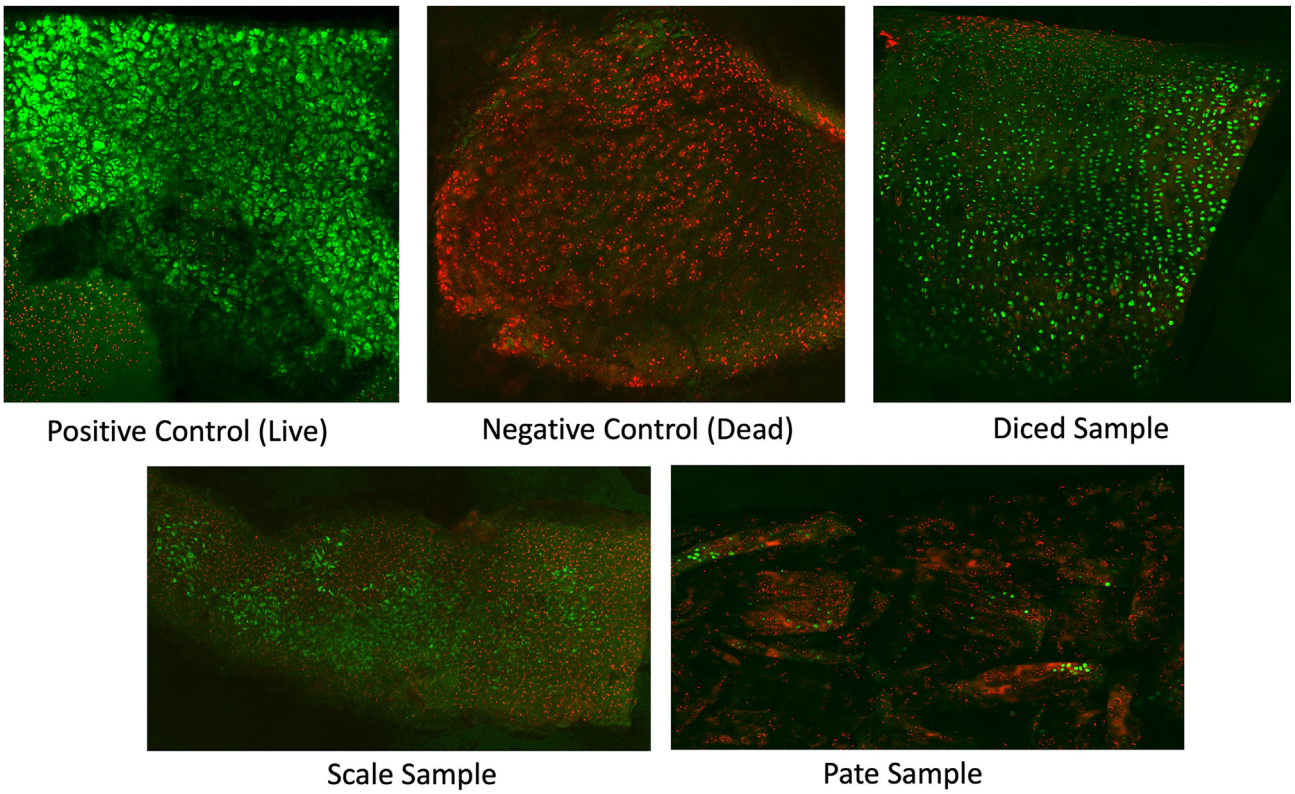

Fig. 2. Photographic examples of viability analysis using the Live/Dead assay and laser scanning confocal microscopy, where green cells signify live chondrocytes whereas red cells signifiy dead chondrocytes. [Color figure can be viewed in the online issue, which is available at www.laryngoscope.com.]

showing the same steep decrease in percent viable cells as the diced cartilage is continuously cut in 0.05 mm increments.

DISCUSSION

Modified cartilage such as finely diced, sliced, crushed, or pate samples are routinely incorporated in

TABLE I.
Bonferroni Post Hoc Analysis of Chondrocyte Viability.

Cartilage Type	Comparison Group	Average % Live Cells	Std. Error	Significance
Alive Control		62.6		
	Dead Control	**1.4**	**0.092**	**<0.001**
	Scale	46.3	0.088	0.945
	Diced	67.8	0.088	0.920
	Pate	**18.3**	**0.080**	**<0.001**
Dead Control		**1.4**		
	Alive Control	**62.6**	**0.092**	**<0.001**
	Scale	**46.3**	**0.088**	**<0.001**
	Diced	**67.8**	**0.088**	**<0.001**
	Pate	18.3	0.080	0.440
Scale		46.3		
	Alive Control	62.6	0.088	0.945
	Dead Control	**1.4**	**0.088**	**<0.001**
	Diced	67.8	0.084	0.158
	Pate	**18.3**	**0.075**	**0.009**
Diced		67.8		
	Alive Control	62.6	0.088	0.920
	Dead Control	**1.4**	**0.088**	**<0.001**
	Scale	46.3	0.084	0.158
	Pate	**18.3**	**0.075**	**<0.001**
Pate		18.3		
	Alive Control	**62.6**	**0.080**	**<0.001**
	Dead Control	1.4	0.080	0.440
	Scale	46.3	0.076	0.009
	Diced	**67.8**	**0.076**	**<0.001**

Bolded values represent statistical significance ($p < 0.05$).

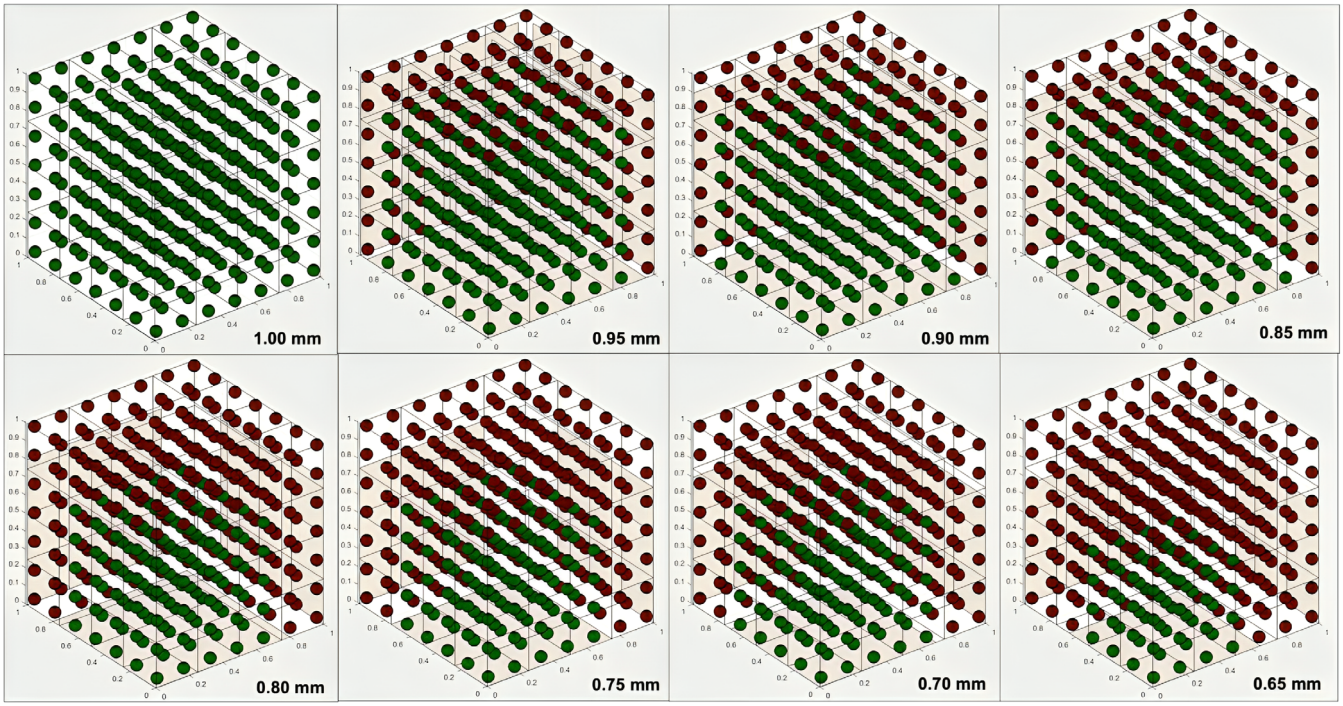

Fig. 3. Computational modeling of diced cartilage with sequential analysis of chondrocyte viability with incremental size decrease, part one. A cube edge length of 0.7–0.8 mm corresponded to 50% chondrocyte viability. [Color figure can be viewed in the online issue, which is available at www.laryngoscope.com.]

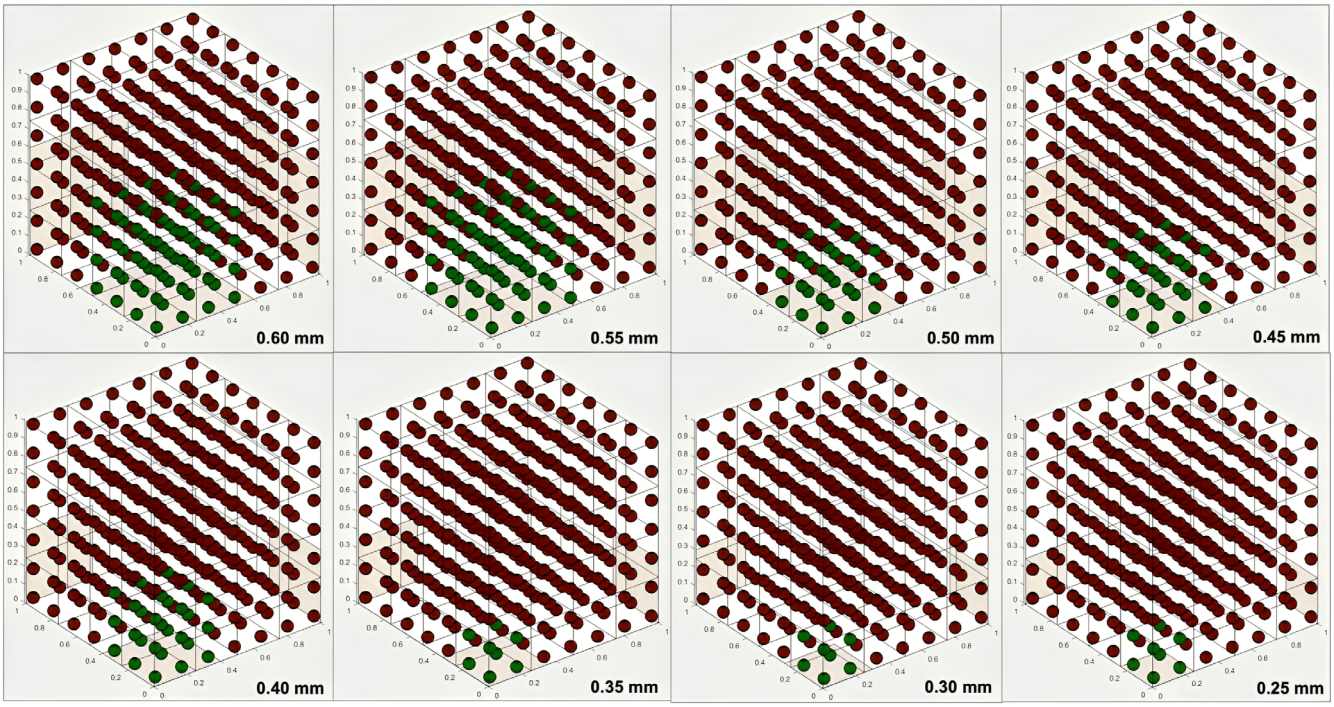

Fig. 4. Computational modeling of diced cartilage with sequential analysis of chondrocyte viability with incremental size decrease, part two. A cube edge length of 0.55–0.65 mm, 25.6% of chondrocytes were viable; at lengths of 0.4–0.5 mm, 10.8% of chondrocytes were viable; and at cube edge lengths of <0.4 mm, less than 5% of chondrocytes were deemed viable. [Color figure can be viewed in the online issue, which is available at www.laryngoscope.com.]

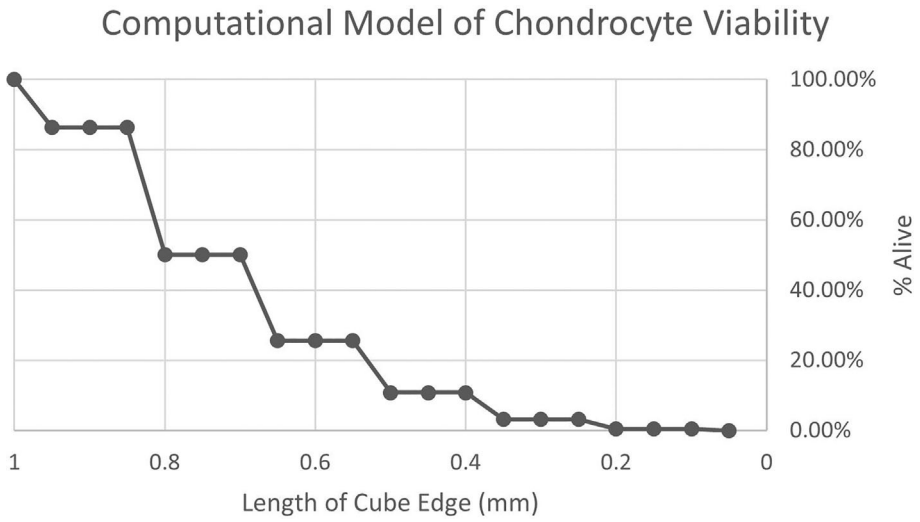

Fig. 5. Results of Figures 3 and 4 in a graphic format, where computational modeling of chondrocyte viability showed a steep decrease of percent viable chondrocytes as the diced cartilage is cut in smaller pieces.

rhinoplasty, and as such this study aimed to evaluate the chondrocyte viability of modified cartilage samples via both live-dead assay and computational model analysis. It was demonstrated that pate/scraped samples had the lowest viability and were similar to formalin immersed samples (negative controls) whereas both 1 mm^3 diced cartilage and 1 mm scaled/shaved cartilage had similar chondrocyte viability as the positive controls. Furthermore, this was the first study to use numerical analysis to estimate changes in percent chondrocyte viability as a function of dicing size. The analysis and figures demonstrated that theoretical chondrocyte viability sharply decreased as the diced cube was cut smaller than 1 mm, with 50% viability correspondence to 0.7–0.8 mm diced cuts, 26% viability in 0.55–0.65 diced cuts, and less than 5% viability in smaller than 0.4 mm diced cuts. With

the popularity of finely diced cartilage, this computational analysis suggests that the potential risk of chondrocyte death increases as diced cartilage is finely cut below 1 mm in size. This can possibly lead to volume loss over time, as viable cells are not present to preserve and maintain the matrix.

In a 2022 study by Dong et al., various-sized diced costal cartilage samples were evaluated after 12 weeks using weight and volume retention rates as well as histopathological and biochemical examinations.[22] They demonstrated that <0.5 mm diced cartilage samples had significant decreases in weight, contour, and chondrocyte nucleus loss compared to 1 mm or 1.5 mm diced cartilage samples. Confocal microscopy was previously performed on auricular cartilage of rabbit models, where Kayabasoglu et al. showed that crushed, diced, and morselized cartilage groups all had significantly less live cell counts than control (unmodified) groups, with crushed cartilage group having the minimum number of viable cells.[12] The negative effects of crushing were also previously demonstrated by Cakmak et al.[11] and Hitzal et al.,[9] where different degrees of crushing (slightly, moderately, severely, and significantly) corresponded to increasing levels of chondrocyte death at tenth day.

The computational analysis of our study showed that as the "cartilage" cube becomes smaller and smaller (increasingly resembling crushed cartilage), viable "chondrocyte" populations decline. Due to the preparation and staining process of Live/Dead assays, it is difficult to examine the change in cell death of the same sample with sequential cuts. Hence, computational modeling facilitates the estimation of cell viability in tissues in a manner that is technically challenging in an experimental setting.[23] This study is the first to perform numerical modeling of these tissue sectioning methods on cartilage tissue viability. The results support previous findings: pate cartilage results in more chondrocyte death than dice (~1 mm), or thinly sliced cartilage. Because significant modification of septal cartilage graft can influence long-term volume loss,[5] surgeons should take caution when incorporating pate or <1 mm diced cartilage into their operations.

Cartilage viability is dependent on a variety of factors beyond just size, which should also be considered when incorporating septal cartilage grafts. Advanced age can significantly decrease glycosaminoglycans, elastin, cell density, and cell size of both auricular and septal cartilages.[24–26] It has been recently suggested that elevating the soft tissue envelope in the sub-superficial musculoaponeurotic system plane had superior chondrocyte viability versus a subperichondrial dissection.[27] Furthermore, implanting cartilage grafts in areas with high tensile forces or increased muscle activity may further lead to volume loss.[2,3] There are also studies reporting high rates of resorption when mixing/wrapping cartilage grafts with AlloDerm, presumably due to mechanisms related to nutrient diffusion.[28,29] These factors should all be considered to balance competing objectives of ideal contour versus ideal volume and shape preservation.

There are some limitations that should be considered when interpreting the present results. First, the number of samples per each group, and thus the power analysis, was limited. Future studies will expand on the number of patients to confirm the statistical significance. Second, the computational analysis could not be exactly correlated with Live/Dead assay microscopic imaging and analysis, simply because precise sectioning below 1 mm with a scalpel is technically challenging, especially beyond 0.7 mm. Furthermore, the positive control samples did not come close to 100% viability, thus there was a moderate amount of cell death in the process besides tissue modification likely limited to the ex vivo nature of specimen procurement. Because the methodology was consistent across the experiment, the results are still interpretable in a relative manner, but regardless, future studies should perform better handling and medium practices. Lastly, the initial dicing of the sample cartilages was done manually using scalpel and rulers, but future studies can do this more precisely and consistently using a cutting jig. Despite these limitations, the study showed the effects of cartilage shape/size modification on chondrocyte viability via both cellular and computational models. In addition to adding to the previous live-dead human chondrocyte viability literature and showing the significant cellular death with pate samples, this study also introduced novel computational modeling to study chondrocyte viability as a function of incremental dicing. This is the first study to suggest significant chondrocyte death as cartilage is diced below 1 mm especially as it is cut below 0.5 mm edges, which invites future studies to validate the findings via live-dead assay.

CONCLUSION

Modifying septal cartilage grafts into 1 mm diced or scaled samples maintains ideal chondrocyte viability whereas the pate preparations result in significant chondrocyte death. Estimated chondrocyte viability sharply decreases as the cartilage is diced below 0.7–0.8 mm, with less than 5% viability at cube edge length below 0.4 mm. Cartilage viability should be considered when preparing modified or thinly diced cartilage in rhinoplasty, which can affect resorption or long-term tissue viability.

ACKNOWLEDGMENTS

This study was made possible in part by access to the Nonlinear Optical Microscopy Lab, part of the Optical Biology Core Facility at UC Irvine, a shared resource supported by the Chao Family Comprehensive Cancer Center (P30CA062203) and the Office Of The Director, National Institutes Of Health award S10OD028698. The study is additionally supported by Leading Foreign Research Institute Recruitment Program through the National Research Foundation of Korea (NRF) funded by the Ministry of Science and ICT (MSIT) (NRF-2022R1l1A3073688), National Institutes Of Health award (NIH), R01 EB030024-01, S10OD028698, GM-076516.

BIBLIOGRAPHY

1. Adamson PA. Grafts in rhinoplasty: autogenous grafts are superior to alloplastic. *Arch Otolaryngol Neck Surg*. 2000;126(4):561-562.

2. Sajjadian A, Rubinstein R, Naghshineh N. Current status of grafts and implants in rhinoplasty: Part I. Autologous grafts. *Plast Reconstr Surg*. 2010;125(2):40e-49e.
3. Bujia J. Determination of the viability of crushed cartilage grafts: clinical implications for wound healing in nasal surgery. *Ann Plast Surg*. 1994; 32(3):261-265.
4. Gassner HG. Structural grafts and suture techniques in functional and aesthetic rhinoplasty. *GMS Curr Top Otorhinolaryngol Head Neck Surg*. 2010;9:1-19.
5. Cakmak O, Buyuklu F. Crushed cartilage grafts for concealing irregularities in rhinoplasty. *Arch Facial Plast Surg*. 2007;9(5):352-357.
6. Dong W, Han R, Fan F. Diced cartilage techniques in rhinoplasty. *Aesthetic Plast Surg*. 2022;46(3):1369-1377.
7. Chang C-S, Bergeron L, Chen PK-T. Diced cartilage rhinoplasty technique for cleft lip patients. *Cleft Palate-Craniofacial J*. 2011;48(6):663-669.
8. Fisher M, Alba B, Ahmad J, et al. Current practices in dorsal augmentation rhinoplasty. *Plast Reconstr Surg*. 2022;149(5):1088-1102.
9. Hizal E, Buyuklu F, Ozer O, Cakmak O. Effects of different levels of crushing on the viability of rabbit costal and nasal septal cartilages. *Plast Reconstr Surg*. 2011;128(5):1045-1051.
10. Cakmak O, Buyuklu F, Yilmaz Z, Sahin FI, Tarhan E, Ozluoglu LN. Viability of cultured human nasal septum chondrocytes after crushing. *Arch Facial Plast Surg*. 2005;7(6):406-409.
11. Cakmak O, Bircan S, Buyuklu F, Tuncer I, Dal T, Ozluoglu LN. Viability of crushed and diced cartilage grafts. *Arch Facial Plast Surg*. 2005;7:21-26.
12. Kayabasoglu G, Ozbek E, Yanar S, et al. The comparison of the viability of crushed, morselized and diced cartilage grafts: a confocal microscopic study. *Eur Arch Oto-Rhino-Laryngology*. 2015;272:1135-1142.
13. Protsenko DE, Ho K, Wong BJF. Survival of chondrocytes in rabbit septal cartilage after electromechanical reshaping. *Ann Biomed Eng*. 2011;39(1):66-74.
14. Badran K, Manuel C, Waki C, Protsenko D, Wong BJF. Ex vivo electromechanical reshaping of costal cartilage in the New Zealand white rabbit model. *Laryngoscope*. 2013;123(5):1143-1148.
15. Pham TT, Heidari AE, Hong EM, et al. Electrochemical lipolysis induces adipocyte death and fat necrosis: in vivo pilot study in pigs. *Plast Reconstr Surg*. Published online May. 2023;153(2):334e-347e.
16. Manuel CT, Foulad A, Protsenko DE, Sepehr A, Wong BJF. Needle electrode-based electromechanical reshaping of cartilage. *Ann Biomed Eng*. 2010;38(11):3389-3397.
17. Molecular Probes TM. *Handbook. A Guide to Fluorescent Probes and Labeling Technologies*. Life Technologies Corporation; 2010.
18. Choi I, Chae Y, Zemek A, Protsenko DE, Wong B. Viability of human septal cartilage after 1.45 μm diode laser irradiation. *Lasers Surg Med off J Am Soc Laser Med Surg*. 2008;40(8):562-569.
19. Vetter U, Heit W, Heinze E, Helbing G, Pirsig W. Growth of the human septal cartilage: cell density and colony formation of septal chondrocytes. *Laryngoscope*. 1984;94(9):1226-1229.
20. Wehland M, Steinwerth P, Aleshcheva G, et al. Tissue engineering of cartilage using a random positioning machine. *Int J Mol Sci*. 2020;21(24):9596.
21. Stockwell RA. Chondrocytes. *J Clin Pathol Suppl (Royal Coll Pathol)*. 1978; 12(7):7-13.
22. Dong W, Wang X, Zhao Z, Fan F. Viability and stability of various-sized free diced cartilage in an experimental study. *Aesthetic Surg J*. 2023;43(3): NP143-NP154, NP143, NP154.
23. Zhu Q, Jackson AR, Gu WY. Cell viability in intervertebral disc under various nutritional and dynamic loading conditions: 3d finite element analysis. *J Biomech*. 2012;45(16):2769-2777.
24. Kim SG, Menapace DC, Mims MM, Shockley WW, Clark JM. Age-related histologic and biochemical changes in auricular and nasal cartilages. *Laryngoscope*. 2024;134(3):1220-1226.
25. Baddam P, Bayona-Rodriguez F, Campbell SM, El-Hakim H, Graf D. Properties of the nasal cartilage, from development to adulthood: a scoping review. *Cartilage*. 2022;13(1):19476035221087696.
26. Riedler KL, Shokrani A, Markarian A, Fisher LM, Pepper J. Age-related histologic and biochemical changes in auricular and septal cartilage. *Laryngoscope*. 2017;127(11):E399-E407.
27. Eravci FC, Kaplan Ö, Oltulu P, et al. The effect of rhinoplasty dissection planes (sub-SMAS, sub-Perichondrial, and sub-periosteal) on the viability of diced cartilage grafts in a rabbit model. *Aesthetic Surg J*. Published online. 2023;43:sjad154.
28. Mola F, Keskin G, Ozturk M, Muezzinoglu B. The comparison of acellular dermal matric (Alloderm), Dacron, Gore-Tex, and autologous cartilage graft materials in an experimental animal model for nasal septal repair surgery. *Am J Rhinol*. 2007;21(3):330-334.
29. Tarhan E, Cakmak O, Ozdemir BH, Akdogan V, Suren D. Comparison of AlloDerm, fat, fascia, cartilage, and dermal grafts in rabbits. *Arch Facial Plast Surg*. 2008;10(3):187-193.